



On dissipative effects of paper web adhesion strength

S. Edvardsson*, P.A. Gradin, P. Isaksson

Division of Applied Mechanics, FSCN, Mid Sweden University, SE-851 70 Sundsvall, Sweden

ARTICLE INFO

Article history:

Received 12 April 2010

Received in revised form 1 September 2010

Available online 15 September 2010

Keywords:

Adhesion strength

Paper web

Peeling test

ABSTRACT

This work is concerned with the adhesion strength between a paper web and a metal roll surface, which is a common situation in paper machines world-wide. It is shown that the classic expression relating the work of adhesion to the peeling angle and web tension is, in general, insufficient. An improved model is suggested to take into account the energy dissipation due to elastic–plastic deformation behavior of wet paper materials. To judge the model, an industrially relevant example of wet newsprint and a mild steel surface is studied. It is found that the agreement between theory and experimental observations is excellent. A key result is that elastic–plastic material behavior must always be included for wet paper materials in peeling processes.

© 2010 Elsevier Ltd. All rights reserved.

1. Introduction

Paper materials are widely used on a daily basis for a variety of goods and services, e.g. printing and packaging qualities or for household needs. Paper essentially consists of a stochastic network of discontinuous cellulose fibers and is usually manufactured by dewatering a cellulose fiber-suspension on a wire. The fibers have an inherent capability to form bonds between them without any additives. Since the fibers are much longer than the thickness of the paper sheet, the network is approximately planar. However, during the manufacturing of paper, the paper web pass through a number of steel rolls on its way from the wet end of the paper machine to the jumbo reel at the other end. When the dry solids content of a paper web is low, i.e. when the paper is wet, the adhesive forces between the rolls and the paper may become significant. A particularly important location in the paper machine where this is crucial is the so-called open draw section, which is situated between the press and the drying section. Here the paper web is transferred between two rolls in which the web frequently becomes loaded by substantial tension variations that frequently lead to web breaks.

There are several causes that may produce unwanted web tension variations. Examples of such causes are: roll materials and their topology as well as the constituents of the paper itself, e.g. quality of utilized wood fibre, moisture content, chemicals etc., cf. (Edvardsson and Uesaka, 2010, 2009; Ahrens et al., 2004; Kurki et al., 2000, 1997). However, the adhesion strength is one of the most paramount factors for the web tension variations in paper machines. In previous works, e.g. (Ahrens et al., 2004; Kurki

et al., 2000, 1997; Mardon et al., 1958; Mardon, 1961, 1976), a simple relation, originally suggested by Rivlin (1944), between web tension and adhesion work was assumed: $G_a = F(1 - \cos\theta_0)$, where G_a is the work of adhesion per unit surface, θ_0 is the peeling angle and F is the web tension (force per unit width). G_a is assumed to be a material constant that needs to be measured and evaluated. However, it turns out that the experimental observation of the peeling tension versus the peeling angle shows that the specific work of adhesion between paper and a given metal surface is not constant as the peeling angle changes (Mardon, 1961). This leads to a suspicion that there might be other dissipative processes involved in the peeling process than solely the work needed to overcome the adhesion forces. In a number of publications, cf. (Kim and Aravas, 1988; Kinloch et al., 1994; Gent and Hamed, 1977; Chang et al., 1972; Williams et al., 2005; Kawashita et al., 2005), plastic bending of polymer films have been considered. In this investigation, an analogous approach for the specific peeling process of paper materials is adopted.

2. The peeling model

Consider a slender cantilever beam with thickness t and unit width as illustrated in Fig. 1. A Cartesian coordinate system is attached to the beam with its origin on the beam's neutral surface. The slope θ at an arbitrary position (x, y) along the beam is given by $\theta = \tan^{-1}[dy/dx]$, where dy/dx is the derivative of y with respect to x . At $x \leq 0$ the beam is clamped whereas the beam at the position (x_0, y_0) is subjected to a tensile force F per unit width directed in the beam's tangential direction (Fig. 1). The bending moment M , per unit width, in the position (x, y) is given by:

$$M = F \cos \theta_0 (y_0 - y) - F \sin \theta_0 (x_0 - x) \quad (1)$$

* Corresponding author.

E-mail address: sverker.edvardsson@miun.se (S. Edvardsson).

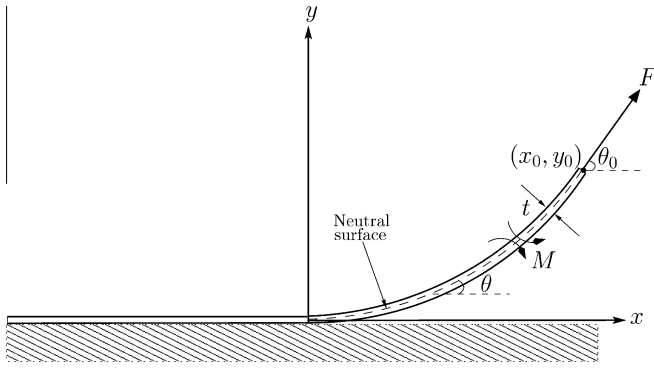


Fig. 1. Slender beam peeled from a metal surface.

where θ_0 is the slope at the position (x_0, y_0) . By taking the derivative of M with respect to θ gives:

$$\frac{dM}{d\theta} = F \left(\sin \theta_0 \frac{dx}{d\theta} - \cos \theta_0 \frac{dy}{d\theta} \right) \quad (2)$$

Let ds denote an infinitesimal length and R the radius of curvature of the beam. Then $ds = R d\theta$, $dx = ds \cos \theta$, $dy = ds \sin \theta$. By introducing the curvature $K = 1/R$, Eq. (2) is rewritten as:

$$K \frac{dM}{d\theta} = F \sin(\theta_0 - \theta) \quad (3)$$

An experimental stress–strain curve, obtained from a uniaxial tensile test performed on a wet newsprint lab sheet paper, is shown in Fig. 2. During the initial loading of the material the response is linear until the yield stress $\sigma = \sigma_0$ is reached. It is noticed that at $\sigma = \sigma_0$ the strain is given by $\varepsilon = \varepsilon_0$. Upon increased loading, the stress–strain response is nonlinear. This behavior is commonly interpreted as that the material is elastic–plastic and the phenomenon that the stress increases with increased plastic deformation, as in Fig. 2, is denoted deformation hardening. Motivated by the re-

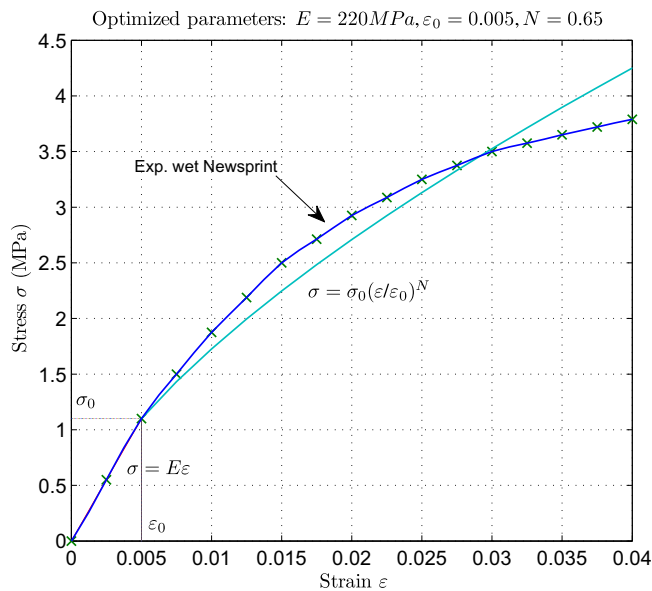


Fig. 2. Stress–strain curve for a wet newsprint sample obtained in a conventional uniaxial tensile test. The width of the sheet is 20 mm and its thickness t is 0.1 mm. Dry solids content is 45% and the testing was performed at the displacement rate of 100 mm/min. Also displayed in the figure is a least-squares fit to a simple material model according to Eq. (4).

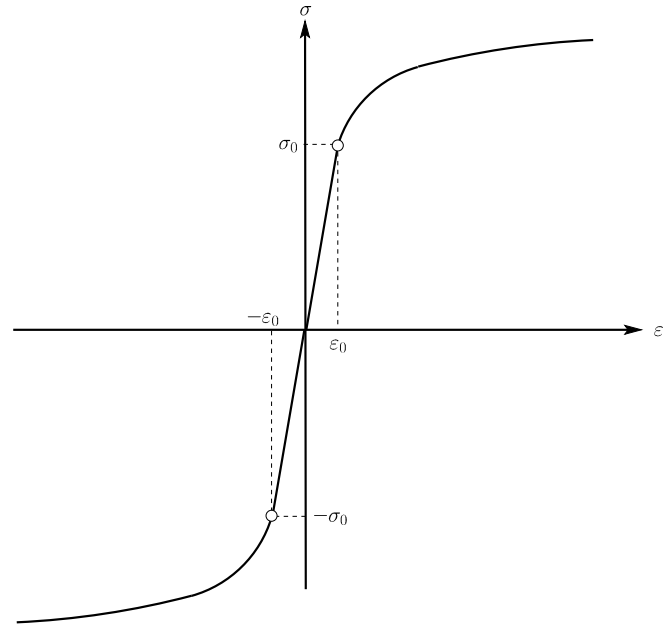


Fig. 3. A symmetric stress–strain relation is assumed (see text).

sult in Fig. 2, it is here assumed that the wet newsprint paper is elastic–plastic and that the stress–strain behavior can be described by a simple relation according to:

$$\begin{cases} \frac{\sigma}{E\varepsilon_0} = \frac{\varepsilon}{\varepsilon_0} & \text{if } \frac{\varepsilon}{\varepsilon_0} \leq 1 \\ \frac{\sigma}{E\varepsilon_0} = \left(\frac{\varepsilon}{\varepsilon_0} \right)^N & \text{else} \end{cases} \quad (4)$$

Here, E is the Young's modulus and N is a hardening exponent ($0 \leq N \leq 1$) which is considered to be a material parameter. If $N = 0$ the material is ideally plastic whereas when $N = 1$ the material is linearly-elastic. Moreover, it is further assumed that the paper material essentially behaves symmetric in tension and compression, Fig. 3, and that the plastic hardening is isotropic, i.e. the yield surface expands equally in tension and compression (these assumptions will be further discussed below). During unloading, reversed plasticity might occur. The strain in the part of the cross section where there is reverse plasticity can be deduced from Fig. 4, i.e., $\sigma(\varepsilon') = -\sigma(\varepsilon)$ implies that $\varepsilon' = 2\varepsilon_B - \varepsilon - 2\sigma_B/E$ so that:

$$\varepsilon' = (2K_B - K)z - 2\sigma_B/E \quad (5)$$

where z is a coordinate in the beam's thickness direction measured from the neutral surface of the material; K_B and K denote the curvatures just before unloading and at an arbitrary instant, respectively. For simplicity, the following dimensionless variables are introduced: $m = M/M_0$ and $k = K/K_e$, where $M_0 = \sigma_0 t^2/4$ and $K_e = 2\sigma_0/Et$. Eq. (3) is then rewritten according to

$$k \frac{dm}{d\theta} = f \sin(\theta_0 - \theta) \quad (6)$$

where $f = 2EF/(\sigma_0^2 t)$ is the normalized tensile force per unit width. The relations between m and k for materials that can be described by Eq. (4) are given by Kim and Aravas (1988):

(a) Elastic loading (O–A):

$$m = \frac{2}{3}k, \quad \text{for } 0 \leq k \leq 1 \quad (7)$$

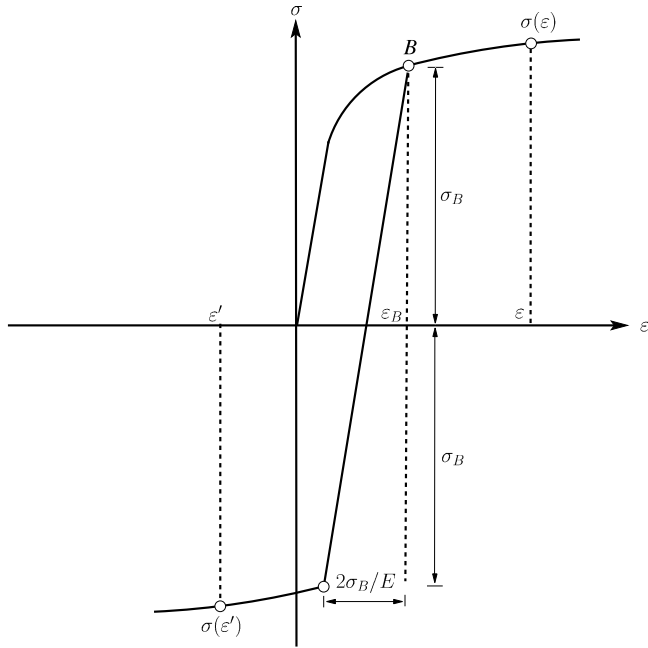


Fig. 4. Model for reversed plasticity effects (see text).

(b) Plastic loading (A–B):

$$m = \left(\frac{2}{3} - \frac{2}{2+N} \right) \frac{1}{k^2} + \frac{2}{2+N} k^N, \quad \text{for } 1 < k \leq k_B \quad (8)$$

(c) Elastic unloading (B–C)

$$m = \left(\frac{2}{3} - \frac{2}{2+N} \right) \frac{1}{k_B^2} + \frac{2}{2+N} k_B^N - \frac{2}{3} (k_B - k), \quad \text{for } k_B \geq k \geq k_B - 2k_B^N \quad (9)$$

(d) Reverse plastic loading (C–D)

$$m = \left(\frac{2}{3} - \frac{2}{2+N} \right) \frac{1}{k_B^2} + \frac{2}{2+N} k_B^N - \frac{2}{3} (k_B - k) \left(\frac{2k_B^N}{k_B - k} \right)^{\frac{3}{1-N}} - \frac{2k_B^N}{2+N} \left[1 - \left(\frac{2k_B^N}{k_B - k} \right)^{\frac{2+N}{1-N}} \right] - I_1(k) \quad (10)$$

for $k_B - 2k_B^N > k \geq 0$, where

$$I_1(k) = 2 \int_{c(k)}^1 \xi \left[(2k_B - k)\xi - 2(k_B \xi)^N \right]^N d\xi$$

and

$$c(k) = \left(\frac{2k_B^N}{k_B - k} \right)^{\frac{1}{1-N}}$$

Here, $c(k)$ is the dimensionless distance from the neutral surface to the interface between the elastic unloading region and the region where reversed plasticity occurs. (Note the printing error in Eq. 10 of Kim and Aravas (1988), where the exponent $(2+N)/(1+N)$ should read $(2+N)/(1-N)$). When a portion da with unit width of the paper web is peeled off, the energy G_{db} da will be dissipated through elastic–plastic bending. The specific dissipation energy G_{db} is given by the area O–A–B–C–D in Fig. 5 multiplied with $M_0 K_e$ (defined below Eq. 5). Now, consider Eq. (6), $kdm/d\theta = f \sin(\theta_0 - \theta)$ together with Fig. 5. On the portion O–A–B, $\theta = 0$ so Eq. (6)

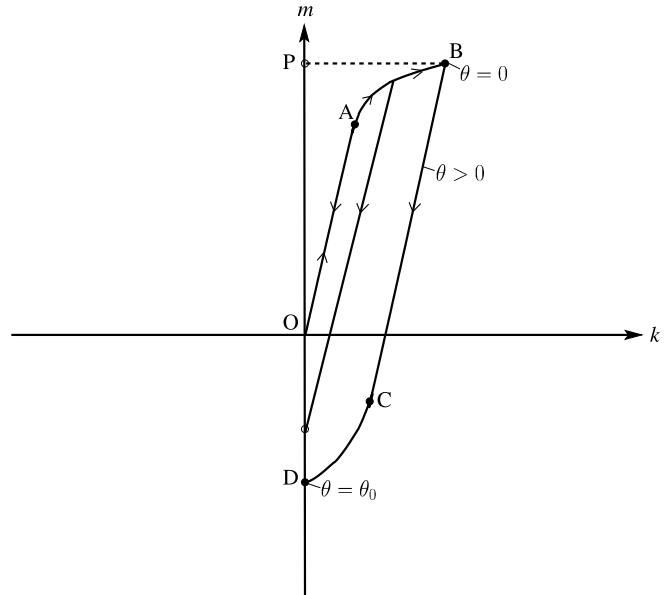


Fig. 5. Bending moment versus web curvature.

is not valid. By integrating Eq. (6) along B–C–D the area O–P–B–C–D is obtained:

$$\text{Area O–P–B–C–D} = f(1 - \cos \theta_0) \quad (11)$$

3. Limitations and additional assumptions

A key question is how the wet paper will behave on the in-plane compressive side of the stress–strain curve. In the literature there are results from compression tests of paper and the conclusion is that the stress/strain at the onset of nonlinear behavior in compression is much less than that for tension (Fellers, 1980; Niskanen, 1998). However, in a situation of in-plane compression, individual fibers in the paper network most likely experience buckling. The conditions in a macroscopic compression test are, however, very far from the conditions experienced by a paper in an adhesion (peeling) test where layers under compression are constrained by layers under tension and fiber buckling is consequently prevented. Hence, as the microscopic fiber buckling is absent, the early loss in stiffness that have been observed in compression tests is expected to be cancelled and the paper material will essentially behave symmetric in tension and compression on the macroscopic scale, Fig. 3. Another question of importance is how the material behaves under unloading from a “plastic” state. Dealing with metal plasticity, it is well-known that unloading from a plastic state, on a macroscopic scale, will be elastic (until reversed plasticity occurs) exhibiting the original Young’s modulus. This elastic behavior (Fig. 4) is also approximately true for the paper materials in various unloading tests, see for example Niskanen (1998).

4. Solution procedure

Three different situations can be identified with reference to Fig. 5. Firstly, if F and θ_0 are such that point A is never reached then there is no elastic–plastic dissipation, i.e. $G_{db} = 0$. The work needed in this situation is solely to overcome the adhesion forces and $G_a = F(1 - \cos \theta_0)$. Secondly, it might also be a situation where plasticity processes are involved during loading but not in the unloading (this situation corresponds to the intermediate line in Fig. 5).

Thirdly, both plastic loading and reversed plasticity processes might be involved.

When the loading situation is such that plasticity is involved during loading but not during unloading, Eqs. (9) and (10) are used to determine the area O–P–B–C–D (see Fig. 5) and by an iterative procedure k_B can then be determined. If $k_B - 2k_B^N \leq 0$ this is the correct solution and Eqs. (7)–(9) can be used to calculate the area between O–A and the intermediate line in Fig. 5, which when multiplied with $Et\epsilon_0^2/2$, gives G_{db} . Otherwise, if $k_B - 2k_B^N > 0$, Eqs. (9) and (10) must be used together with Eq. (11) to determine, by iterations, the value of k_B so that G_{db} then can be calculated by using Eqs. (7)–(10). Finally, the value of the specific adhesion work is determined by:

$$G_a = F(\theta_0)(1 - \cos \theta_0) - G_{db}(\theta_0) \quad (12)$$

5. Evaluation of experimental observations

A peeling experiment for wet newsprint is provided in Fig. 6 (top panel). The experiment was performed for a lab sheet having dry solids content 36% (Mardon, 1961). First an analysis is performed by assuming that the material is linearly-elastic. In this case, the bending moment is given by the linear relation $M = K\epsilon t^3/12$. Eq. (3) readily gives $K^2 = 24F \frac{(1 - \cos(\theta_0 - \theta))}{\epsilon t^3}$, where the condition that $K = 0$ at $\theta = \theta_0$ has been utilized. The maximum curvature is at $x = 0$, where $\theta = 0$, i.e. $K_{max} = \sqrt{24F(1 - \cos \theta_0)/(Et^3)}$. Since the maximum strain over the cross section in this case is given by $Kt/2$, the largest strain ϵ_{max} in the whole structure is given by:

$$\epsilon_{max} = \sqrt{6F(1 - \cos \theta_0)/(Et)} \quad (13)$$

By applying Eq. (13) to the experimentally measured values (Fig. 6) we note that $\epsilon_{max} > 2\%$ for all the studied peeling angles θ_0 (lower panel). However, according to stress–strain results in Fig. 2, inelastic behavior initiates already for $\epsilon \gtrsim 0.5\%$. In the case of wet newsprint, the bending is therefore always inelastic. Thus, the classic relation widely in use for the specific work of adhesion, $G_a = F(1 - \cos \theta_0)$, is insufficient for wet newsprint. This discrepancy is also generally seen for all the various paper materials studied in Ref. (Mardon, 1961). This observation is in fact an important motivation for carrying out this study. Another question is if it is really sufficient to include only plastic bending behavior, or if also plastic tensile (longitudinal) effects need to be accounted for. In Fig. 2 it is seen that at $\epsilon = 0.5\%$ the tension is 110 N/m. All the tension values in Fig. 6 (top) are much smaller so longitudinal plasticity will not occur in the present study.

In Fig. 7 the case of newsprint with 36% dry solids content and a mild steel surface is shown (experimental results from Fig. 19 of Mardon (1961)). By assuming $F(\theta_0) = G_a/(1 - \cos \theta_0)$ the best, in a least-square sense, fit is obtained for $G_a = 1.5 \text{ J/m}^2$. Although the fit certainly can be improved for the larger angles it would then become worse for the smaller angles. Hence, we note that the agreement based on this adhesion model is very poor. In fact, the general limitation of the elastic expression, $G_a = F(\theta_0)(1 - \cos \theta_0)$, could already be seen in Mardon's work in 1961 (Mardon, 1961). The assumed θ_0 -dependence may be studied by a Taylor expansion according to $F(\theta_0) = G_a/(1 - \cos \theta_0) \approx 2G_a/\theta_0^2$ which is reasonable for relatively small angles θ_0 . However, the experimental findings clearly show that in addition to a $1/\theta_0^2$ -dependence, there is also a strong angular $1/\theta_0$ -component present. This is manifested by the observation that the theoretical curve is always declining much faster than the experimental ditto, see Fig. 7 and (Mardon, 1961). Moreover, for the larger angles, $F(\theta_0)$ turns upwards (Fig. 7), a property that is inconsistent with the assumption that $F(\theta_0) = G_a/(1 - \cos \theta_0)$.

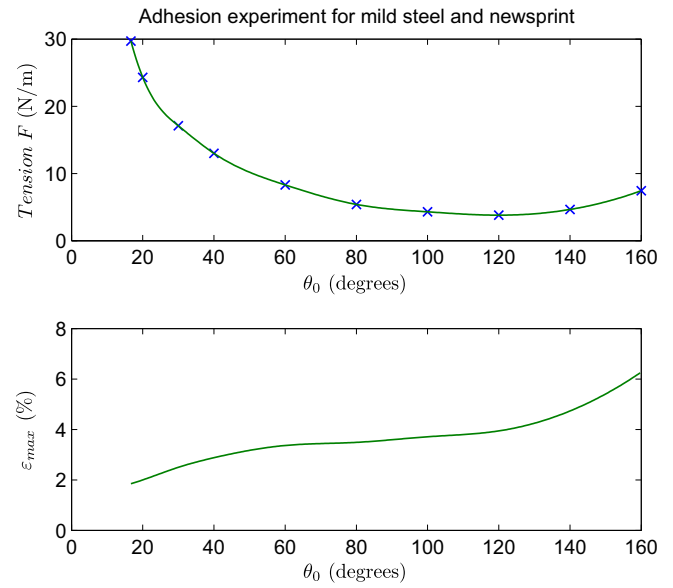


Fig. 6. The top panel shows experimental values for mild steel and newsprint with 36% dry solids content from Mardon (1961). The lower panel shows the corresponding maximum strain ϵ_{max} in the structure, i.e. Eq. (13). Material parameters used are $E = 220 \text{ MPa}$ and $t = 0.1 \text{ mm}$ (from Fig. 2).

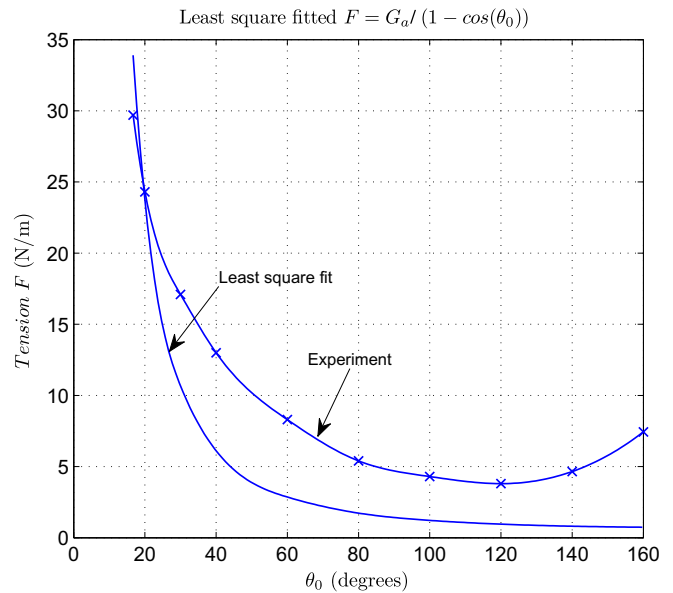


Fig. 7. The top curve is experimental values for mild steel and newsprint from Mardon (1961) (see text). The lower curve is the classic model (Rivlin, 1944), fitted in a least-square sense, to the experiment resulting in $G_a = 1.5 \text{ J/m}^2$.

In order to apply the adhesion model suggested here, a value for the specific work of adhesion G_a is needed (here considered to be a system constant). This can be achieved by expanding Eq. (12) and write $F(\theta_0) = 2(G_a + G_{db}(\theta_0))/\theta_0^2$. From the application of Eqs. (7)–(10) we find that $G_{db}(\theta_0) = k\theta_0$ is well fulfilled for relatively small θ_0 . This is also consistent with the fact that $G_{db}(\theta_0) \rightarrow 0$ as $\theta_0 \rightarrow 0$, since then m and k become negligible (i.e., the elastic case in Fig. 5). Thus we may write $F(\theta_0) = 2G_a/\theta_0^2 + 2k/\theta_0$. It is interesting to note that the missing angular $1/\theta_0$ -component noted above is indeed present in the current theory and by rearranging one obtains the specific work of adhesion: $G_a = \theta_0^2/2[F(\theta_0) - 2k/\theta_0]$. The lowest measured angle, $\theta_0 = 16.7^\circ$, and its corresponding measured force F

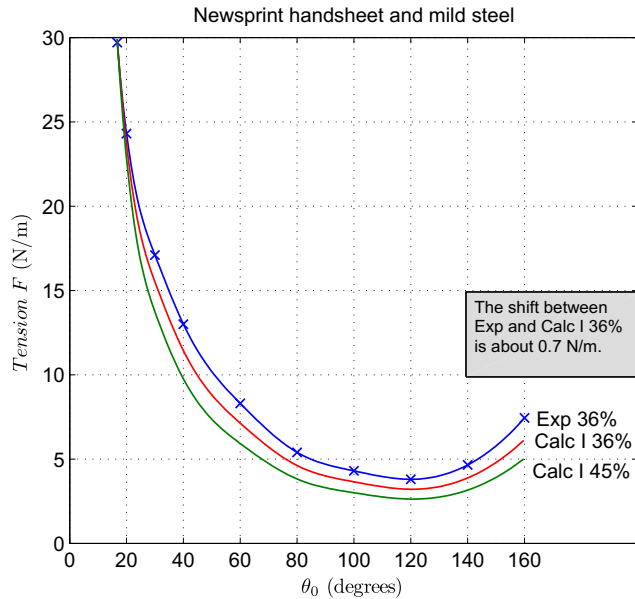


Fig. 8. Account for moisture. The term “Calc I” refers to the application of the Eqs. (7)–(10).

are used to evaluate the value of G_a (k is easily determined in the numerical evaluation of $G_{db}(\theta_0)$).

In Fig. 8, a comparison between the theoretical results of Eqs. (7)–(10) and (12), and the experimental result is shown. The lowest curve in Fig. 8 is the result for newsprint at 45% dry solids content (from Fig. 2). Since the experimental result in Fig. 8 is for 36%, we do not expect a perfect agreement. Still the general curve shape is promising. For example, the upturn beyond 120° is well represented. In order to improve the comparison, we have estimated the following material parameters for newsprint having 36% dry solids content: $E=80$ MPa, $\varepsilon_0=0.003$, $N=0.5$ and $t=0.115$ mm. The result of this is shown in Fig. 8 as the centre curve. It is seen that even though there is a considerable improvement, there is still a discrepancy left. A further adjustment of the material parameters was made to improve the fit. However, it turned out that a perfect

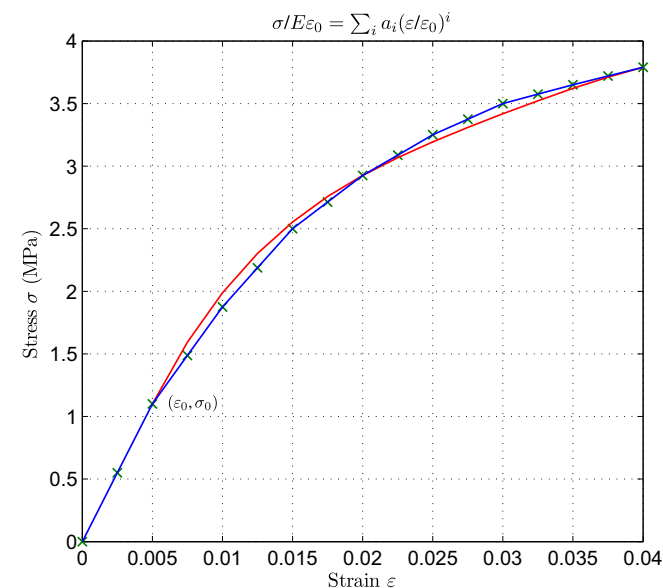


Fig. 9. Improved material model, see the Appendix.

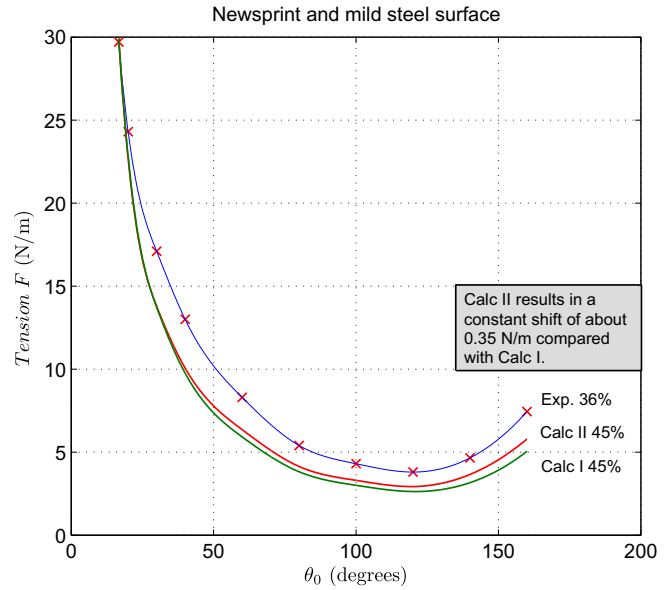


Fig. 10. Comparison between successively improved models. The term “Calc II” refers to the application of the Eqs. (A.2)–(A.5) in the Appendix. In the case Calc II 45%, reverse plasticity occurs for peeling angles $\theta_0 > 50^\circ$ (see C–D in Fig. 5) and the work of adhesion $G_a = 0.93$ J/m². In the case of loading, plastic effects are present for all the peeling angles studied ($\theta_0 > 16.7^\circ$).

match could not be achieved by requiring that the parameters still were kept within realistic ranges. A plausible explanation for the discrepancy could be that the assumed material model, i.e. Eq. (4), is not sufficiently flexible. In fact, it is indeed seen in Fig. 2 that the material model only approximately reflects the experimental reality. Therefore, in the Appendix an improved material model, Eq. (A.1), is provided. As can be seen in Fig. 9, the agreement becomes significantly improved. In order to recalculate the peeling tension versus peeling angle, the expressions of Eqs. (7)–(10) are modified according to Eqs. (A.2)–(A.5) given in the Appendix. The improvement of this (“Calc II”) is shown in Fig. 10 in the case of 45% dry solids content ($G_a = 0.93$ J/m²). Basically, the improvement constitutes of a shift of 0.35 N/m in the correct direction. By keeping in mind that the theoretical curve is for 45% and not 36%, the estimated parameters for 36% newsprint are applied (see above). A theoretical curve is then obtained that is in good agreement with the experiment except for a constant shift of 0.7 N/m (applied in Fig. 11). This constant shift may very well be due to a systematic calibration error in the original force measurements in Ref. (Mardon, 1961) or due to various approximations in the applied model. One possibility may be the idealized assumption (near Eq. (13)) that $\theta = 0$ at $x = 0$. This assumption can be relaxed by introducing an intermediate layer between the paper web and the steel surface (root rotation), see e.g. (Williams et al., 2005; Kawashita et al., 2005). Another possibility might be the influence from gravity on the tension. This is of the order mlg , where $m \approx 0.1$ kg/m² is the grammage, $l > 0.1$ m is the paper length above the metal surface and $g \approx 10$ m/s² is the acceleration of gravity, thus $mlg > 0.1$ N/m which is the same order of magnitude as the constant shift. The usual velocity term mv^2 , however, is negligible because the test velocity $v \sim 0.1$ m/s or less, so $mv^2 < 10^{-3}$ N/m. Thus, we conclude that there is no essential deviation between the model and the experimental observations, which provides strong confidence for the suggested model.

Finally, in Fig. 12 the ratio between the classic and current peeling theory, which is given in the Appendix, is shown. The calculation of G_{db} depends on the experimental values of F (through Eq. 11

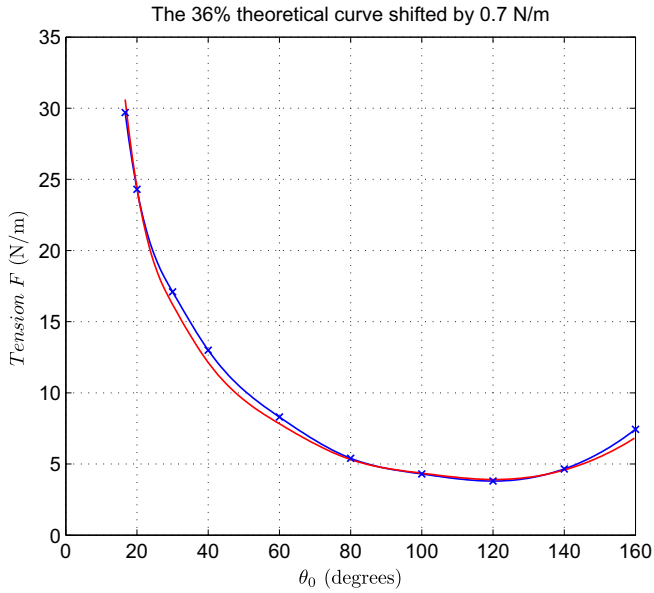


Fig. 11. Final “Calc II” results estimated for 36% dry solids content and the corresponding experimental data (crosses).

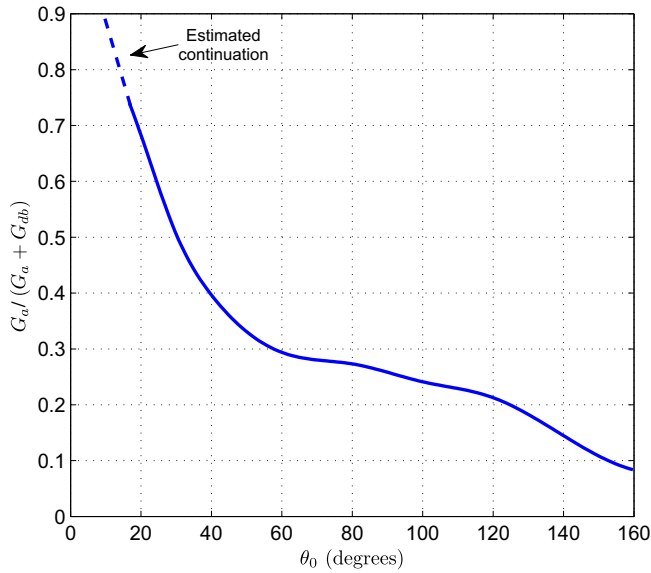


Fig. 12. The curve shows the ratio between the classic and current peeling theory (given in the Appendix). The calculation is made for a newsprint sample with 45% dry solids content for which $G_a = 0.93 \text{ J/m}^2$. The classic model is acceptable at about 10° or lower for which the relative error is less than 10%.

which is needed to determine k_B). The experiment is only available down to 16.7° , so for the lower angles only an estimation can be made, see Fig. 12. In any case, at $\theta_0 = 10^\circ$ it is indicated that the classic model is reasonably accurate since the relative error is only about 10%. For lower angles θ_0 , the curvature is small so that the plastic effects due to bending vanishes. However, for the larger peeling angles the situation worsens considerably. For example, above 30° the relative error is greater than 50%. In the case of very small peeling angles, both the classic model and the suggested model may become inaccurate because at tiny angles the peeling force F becomes large and might be substantial enough so that longitudinal plastic effects no longer can be neglected. As already

noted, this problem occurs if F exceeds 110 N/m (in the case of dry solids content of 45%).

6. Conclusions

It is found that the classic adhesion model frequently used in applied research and particularly in the paper industry is inaccurate. When applied to paper materials, the classic peeling model is questionable because its predictions severely disagrees with experimental observations. In the present work, a more general adhesion model for paper webs is developed which agree very well with experimental findings. The presented results also indicate that the work of adhesion G_a is constant (i.e., independent of the peeling angle). Therefore it is, for the first time, possible to estimate the true G_a for various surfaces and wet paper materials. It is hoped that this adhesion model turns out to be useful in future works dealing with peeling tests, simulations and interpretations of paper web dynamics.

Acknowledgments

Financial support from the Swedish Research Council and the KKS-foundation are greatly acknowledged.

Appendix A

The relations between m and k (Eqs. (7)–(10)) for materials defined by Eq. (4) are here improved according to a more accurate material model:

$$\begin{cases} \frac{\sigma}{E\epsilon_0} = \frac{\epsilon}{\epsilon_0}; & \frac{\epsilon}{\epsilon_0} \leq 1 \\ \frac{\sigma}{E\epsilon_0} = \sum_{i=0}^4 a_i \left(\frac{\epsilon}{\epsilon_0}\right)^i; & \frac{\epsilon}{\epsilon_0} > 1 \end{cases} \quad (\text{A.1})$$

where the parameters a_i are fitted to the experimental curve in Fig. 2. The result of this is shown in Fig. 9.

(a) Elastic loading (O–A):

$$m = \frac{2}{3}k, \text{ for } 0 \leq k \leq 1 \quad (\text{A.2})$$

(b) Plastic loading (A–B):

$$m = \frac{2}{3k^2} + 2 \sum_i a_i \frac{k^i}{i+2} \left(1 - \frac{1}{k^{i+2}}\right), \text{ for } 1 < k \leq k_B \quad (\text{A.3})$$

(c) Elastic unloading (B–C)

$$m = m_B - \frac{2}{3}(k_B - k), \text{ for } k_B \geq k \geq k_C \quad (\text{A.4})$$

where $k_C = k_B - 2 \sum_i a_i k_B^i$; and m_B is obtained from Eq. (A.3) with $k = k_B$.

(d) Reverse plastic loading (C–D)

$$m = m_B - \frac{2}{3}(k_B - k)c(k)^3 - 2 \sum_i a_i \frac{k^i}{i+2} \left(1 - c(k)^{i+2}\right) - 2I_1(k) \quad (\text{A.5})$$

for $k_C > k \geq 0$, where $c(k)$ is obtained by solving $c(k)(k_B - k) = 2 \sum_i a_i (k_B c(k))^i$ iteratively and

$$I_1(k) = \int_{c(k)}^1 \sum_r a_r \left[(2k_B - k)\xi - 2 \sum_i a_i (k_B \xi)^i \right]^r \xi d\xi$$

References

- Ahrens, F., Patterson, T., Bloom, F., 2004. *Int. J. Appl. Mech. Eng.* 9, 227.
- Chang, M.D., Devries, K.L., Williams, M.L., 1972. The effects of plasticity in adhesive fracture. *J. Adhesion* 4, 221.
- Edvardsson, S., Uesaka, T., 2009. System stability of the open draw section and paper machine runnability. *FRC Symp.*, Oxford 1, 557.
- Edvardsson, S., Uesaka, T., 2010. System dynamics of the open-draw with web adhesion: particle approach. *J. Appl. Mech.* 77, 021009.
- Fellers, C., 1980. The Significance of Structure on the Compression Behaviour of Paper. Doctoral Dissertation. Royal Institute of Technology, Stockholm.
- Gent, A.N., Hamed, G.R., 1977. Peel mechanics for an elastic–plastic adherend. *J. Appl. Polymer Sci.* 21, 2817.
- Kawashita, L.F., Moore, D.R., Williams, J.G., 2005. Analysis of peel arm curvature for the determination of fracture toughness in metal–polymer laminates. *J. Mat. Sci.* 40, 4541.
- Kim, K.-S., Aravas, N., 1988. Elastoplastic analysis of the peel test. *Int. J. Solids Struct.* 24, 417.
- Kinloch, A.J., Lau, C.C., Williams, J.G., 1994. The peeling of flexible laminates. *Int. J. Fract.* 66, 45.
- Kurki, M., Pakarinen, P., Juppi, K., Martikainen, P., 2000. In *Papermaking part 2: Drying*. Fapet Oy.
- Kurki, M., Vestola, J., Martikainen, P., Pakarinen, P., 1997. 1997 Proc. of 4th Int. Conf. of Web Handling, 527.
- Mardon, J., 1961. *Appita* 15, 14.
- Mardon, J., 1976. *Papper och Trä* 11, 797.
- Mardon, J., Truman, A.B., O'Blens, G., Meadley, K., 1958. *Pulp and Paper Magazine of Canada* (Sept), 135.
- Niskanen, K., 1998. *Paper Physics (Papermaking Science and Technology)*. OY, Helsinki, Finland.
- Rivlin, R.S., 1944. *Paint Technology* 9, 215.
- Williams, J.G., Hadavinia, H., Cotterell, B., 2005. Bending solution for edge constrained beams. *Int. J. Solids Struct.* 42, 4927.